Top Catal (2015) 58:887–895
DOI 10.1007/s11244-015-0455-0

ORIGINAL PAPER

Characterisation and Catalytic Fischer–Tropsch Activity of Co–Ru and Co–Re Catalysts Supported on γ-Al_2O_3, TiO_2 and SiC

H. Romar[1,3] · A. H. Lillebø[2] · P. Tynjälä[1,3] · T. Hu[1,3] · A. Holmen[2] · E. A. Blekkan[2] · U. Lassi[1,3]

Published online: 11 August 2015

Abstract A number of supported cobalt catalysts for Fischer–Tropsch synthesis were considered. Catalysts were prepared by impregnation of the supports with a cobalt precursor resulting in cobalt concentrations of 15 or 20 wt%. The active metal was supported onto aluminum oxide, titanium dioxide and silicon carbide supports while rhenium or ruthenium metals were used as promoters, whose concentrations were 0, 0.2 or 1.0 wt%. The catalysts were characterized by a number of methods including BET, chemisorption, and XRD. Some of the catalysts were tested for catalytic activity and selectivity in the Fischer–Tropsch reaction using a fixed bed reactor. Based on the results, the addition of promoter metals increases the dispersion of the active metal cobalt and correspondingly a decrease in the cobalt metal particles, this effect was most evident for the alumina supported catalysts. Further, increased concentrations of the ruthenium promoter (1.0 wt%) slightly increased the selectivity to CH_4 and decreased selectivity to C_{5+}.

Keywords Catalyst · Cobalt · Alumina · Titanium dioxide · Silicon carbide · Fischer–Tropsch · XRD · Activity

✉ H. Romar
henrik.romar@chydenius.fi

[1] Department of Applied Chemistry, Kokkola University Consortium Chydenius, University of Jyvaskyla, P.O. Box 567, 67101 Kokkola, Finland

[2] Department of Chemical Engineering, Norwegian University of Science and Technology (NTNU), 7491 Trondheim, Norway

[3] Research Unit of Sustainable Chemistry, University of Oulu, P.O. Box 3000, 90014 Oulu, Finland

1 Introduction

There is a growing interest to find new chemicals to replace the fossil-based traffic fuels presently used. One such solution is thermochemical conversion of biomass under restricted oxygen supply (gasification) to synthesis gas [1–4]. The resulting gas, synthesis gas or syngas can, after proper cleaning procedures, be converted by a catalytic process; the Fischer–Tropsch synthesis (FTS), into a number of chemicals, among them traffic fuels. FTS produces a mixture of hydrocarbons ranging in chain lengths from methane to long chained, solid or semisolid, waxes. The composition of the product mixture from FTS depends on a number of factors such as active and promoting metals used in the catalyst, temperature and pressure used for the reaction and the composition of the syngas used. One important factor is the ratio of H_2 to CO in the syngas. Cobalt based catalysts are usually operated at a H_2 to CO ratio of 2 but usually the ratio is much lower especially in biomass derived syngas where it is 1:1 or even lower. The most interesting compounds formed in the FTS are the ones that are present in liquid or semi-solid state, C_{5+} and waxes especially, because these compounds can easily be used as such or they can be converted to traffic fuels [5–7].

Iron (Fe) and cobalt (Co) catalysts have often been used in FTS. These catalysts can be prepared using methods like precipitation or impregnation. Usually the active metals are added onto supports, i.e. aluminum oxide (Al_2O_3), titanium dioxide (TiO_2) and silicon dioxide (SiO_2) but also other supports like ceria based compounds and silicon carbide have been tried. Besides the active metal, usually cobalt or iron, some promoting metals like platinum, ruthenium, rhodium and rhenium are added to the catalysts in small amounts (<1.0 wt%) in order to increase the dispersion of the active metal and to make more of the metal accessible

for the gas thereby increasing the activity of the catalyst. The addition of the promoter metals also enhances the reduction of the active metals, especially at lower temperatures. This reduction effect is the most important effect of promoter metals regarding aluminum supported cobalt catalysts. In some cases, the promoters also have an impact on the transfer of electrons between the support and the active metal [2, 8, 9].

In this study a series of cobalt catalysts were prepared on three different supports; aluminum oxide (Al_2O_3), titanium dioxide (TiO_2) and silicon carbide (SiC). To some of the catalysts the promoter metals ruthenium (Ru) or rhenium (Re) were added in concentrations of 0, 0.2 or 1.0 mass%. Catalysts are characterized by a number of methods and the most promising catalysts are tested for activity and selectivity in the Fischer–Tropsch reaction.

2 Materials and Methods

2.1 Catalysts and Catalyst Preparation

In this research a series of Co catalysts for Fisher–Tropsch synthesis were produced and characterized. Catalysts were supported by different supports; aluminum oxide (Al_2O_3, γ-phase, Puralox SCCa 5/200, provided by Sasol, Germany), titanium dioxide (TiO_2 Degussa P25) and β-silicon carbide (SiC provided by SiCatCatalysts). Properties for the supports used in this study are presented in Table 1. The cobalt catalysts were prepared by a one-step incipient wetness-impregnation process, where Al_2O_3 and TiO_2 were used as delivered, while SiC pellets were milled and sieved (50-100 μm fraction size) before being used for impregnation. The following precursor salts, or in one case solution, of the precursors were used: $(Co(NO_3)_2{\cdot}6H_2O$, $Ru(NO)(NO_3)_2$ and perrhenic acid ($HReO_4$). Prior to impregnation all supports were dried at 80 °C for 2 h. The precursors were dissolved in distilled water giving volumes equal to the pore volumes of the supports as described by the manufacturers. The impregnations were performed by mixing supports and precursors in a one-step process for 16 h with continuous stirring. After mixing the catalysts were dried, first at sub-atmospheric pressure for 30 min followed by drying in an oven at 105 °C for 2 h. In order to break down the precursor salts the dried catalysts were calcined at 420 °C for 16 h in static atmosphere. For the unimpregnated supports the same calcination process was used. The calcined catalysts were crushed and sieved, fractions 50–100 μm in size were used for further characterizations.

Catalysts used in this study are denoted as follows: support-cobalt content-ruthenium or rhenium content. Supports are abbreviated with the following symbols: A = Al_2O_3, S = SiC and T = TiO_2. Therefore, e.g. catalyst denoted A20Re0.2 contains 20 wt% Co and 0.2 wt% rhenium supported on Al_2O_3.

Calcined catalysts were characterized by a number of techniques: surface area and pore size distribution measurements were performed by nitrogen physisorption, metal dispersion by CO chemisorption, metal content by ICP and X-ray diffraction (XRD). For some of the alumina based catalysts, the activity and selectivity in the Fischer–Tropsch reaction was determined.

2.2 Catalyst Characterization

2.2.1 Specific Surface Area and Pore Distribution

Portions of each catalyst (about 200 mg) were pretreated at low pressures and high temperatures in order to clean their surfaces, the measurements were made with calcined but unreduced samples. The pretreatment was performed by heating the sample to 50 °C with a rate of 10 °C/min, at this stage the pressure was dropped to 5 mm Hg at a rate of 5 mm Hg/s. After stabilization at 50 °C, the temperature was elevated to 140 °C using the same ramp as previous, pressure was lowered to 10 μm Hg. Samples were kept at 140 °C and 10 μm Hg for 120 min. Adsorption isotherms were obtained by immersing sample tubes in liquid nitrogen (−196 °C) in order to obtain isothermal conditions. Nitrogen was added to the samples in small steps and the resulting isotherms were obtained. Specific surface areas were calculated from adsorption isotherms according to the Brunauer–Emmett–Teller method (BET). Nitrogen adsorption and desorption isotherms were used to calculate the pore size distribution using the method proposed by

Table 1 Properties of supports used in the study (information provided by the suppliers)

Support		Surface area (m^2/g)	Pore volume (cm^3/g)	Average pore diameter (nm)
Al_2O_3	Sasol Puralox SCCa	195	0.52	10.6
SiC	Sicat β-SiC UHP3 LO	25	0.15	24.0
TiO_2	Degussa Aerosile P-25	54	0.18	13.5

Barrett–Joyner–Halenda (BJH). The determinations were performed using a Micromeritics ASAP 2020 instrument. Precision for the BET surface analysis is reported to be ±5 % when measured on standard substances [10].

2.2.2 Chemisorption

About 500 mg of each catalyst was weight into a U-shaped quartz glass tube in which the sample was supported on both sides by quartz wool. The samples were evacuated and reduced in a flow of H_2, first at a temperature of 110 °C for 30 min followed by reduction at 350 °C for 2 h. Temperature rise was 10 °C/min. Following the reduction of samples the temperature was lowered to 40 °C, and the tubes evacuated which allowed small pulses of CO to be adsorbed onto the Co surface. The metal dispersions and sizes of the Co metal particles were calculated by assuming the stoichiometry of 2:1 between Co and CO. Chemisorption measurements were performed using a Micromeritics ASAP 2020.

2.2.3 XRD

Prior to analysis the samples were reduced at 350 °C for 3 h in a H_2 atmosphere with a flow rate of 65 mL/min, and the subsequent crystalline phases and structures were analyzed by XRD. XRD patterns were recorded by a Siemens D5000 X-ray diffractometer using monochromatic Cu Kα radiation (λ = 1.5418 Å) at 40 kV and 30 mA at the Center of Microscopy and Nanotechnology at the University of Oulu. The average crystallite size (D) of the samples was determined according to the Scherrer equation (Eq. 1).

$$D_p = \frac{K\lambda}{\beta_{1/2}\cos\theta} \quad (1)$$

In Eq. 1, K = 0.9, $\lambda_{K\alpha} = 0.15418$ nm, βc is full width high medium and θ is the Bragg angle for the considered peak [11].

2.2.4 Metal Content by ICP

Some of the catalysts were analyzed for metal content by inductively coupled plasma optical emission spectroscopy (ICP-OES, Perkin Elmer Optima 5300 DV). A portion of each catalyst (about 100 mg) was digested in a microwave oven using an acid mixture containing 9 ml concentrated HCl and 1,5 ml concentrated HNO_3 to dissolve the metals. The digestion was performed at 200 °C with a temperature ramp of 15 min (about 12 °C/min) and a hold time at 200 °C for 10 min. The final solution was diluted to 50 ml with ultrapure water before analysis. Besides analysis of the active and promoter metals, catalysts were also analyzed for sodium and potassium contents too. No suitable standard was available for Ru measurements, and therefore no data is available for this element.

2.3 Activity and Selectivity Measurements

Activity and selectivity measurements were performed for some catalysts. The measurements were carried out in a fixed-bed tubular reactor (Fig. 1). 1 g of calcined catalyst, sieved to a particle size of 50–100 μm, was carefully mixed with 15 grams of silicon carbide (SiC) and packed into the middle of the fixed bed reactor. The catalyst bed was supported on both sides by glasswool. Catalysts were reduced in the reactor tube in a flow of hydrogen at 350 °C for 16 h (temperature ramp 100 °C/h). After the reduction step the reactor was cooled down to 180 °C and pressurized to 20 Bar with nitrogen whereupon the flow was switched to syngas (3.1% N_2, 31% CO, H_2 65.9 %; AGA Special gases) with an initial flow of 250 ml/min.

Temperature was slowly elevated from 180 °C; first with 10 °C/h to 200 °C, from 200 to 205 °C the temperature was elevated with 5 °C/h, finally the temperature was manually elevated in small increments to 210 °C. Temperature inside the catalyst bed was measured with a movable thermo element (K-type) inserted into a pocket inside the reactor. This element was used in the final stage to fine-tune the temperature to 210 °C over the whole catalyst bed.

The reactor was kept with a flow rate of 250 ml/min for 24 h. After this initial stabilization period, the flow was then adjusted to give a CO conversion of 50 % calculated from the CO/N_2 peaks obtained from a gas chromatograph (Agilent 7890 with TCD and FID) connected on-line to the reactor. Liquids and semi-solid products were collected in two traps, one heated to 90 °C for heavier waxes and water (hot trap) and one kept at ambient temperature for light liquid compounds (cold trap). Gaseous compounds present after the second trap were measured with the on-line GC. Integrated signals from the GC were later used for the calculation of activity and selectivity of each catalyst.

3 Results and Discussion

3.1 Characterization of Catalysts

All the catalysts were characterized by physisorption and chemisorption while the specific surface areas were measured by the BET method, the results are presented in Table 2. The surface areas after impregnation of Co and promoter metals are as expected lower than the corresponding values for the calcined supports. This indicates a partial or even total blockage of some pores. Most likely

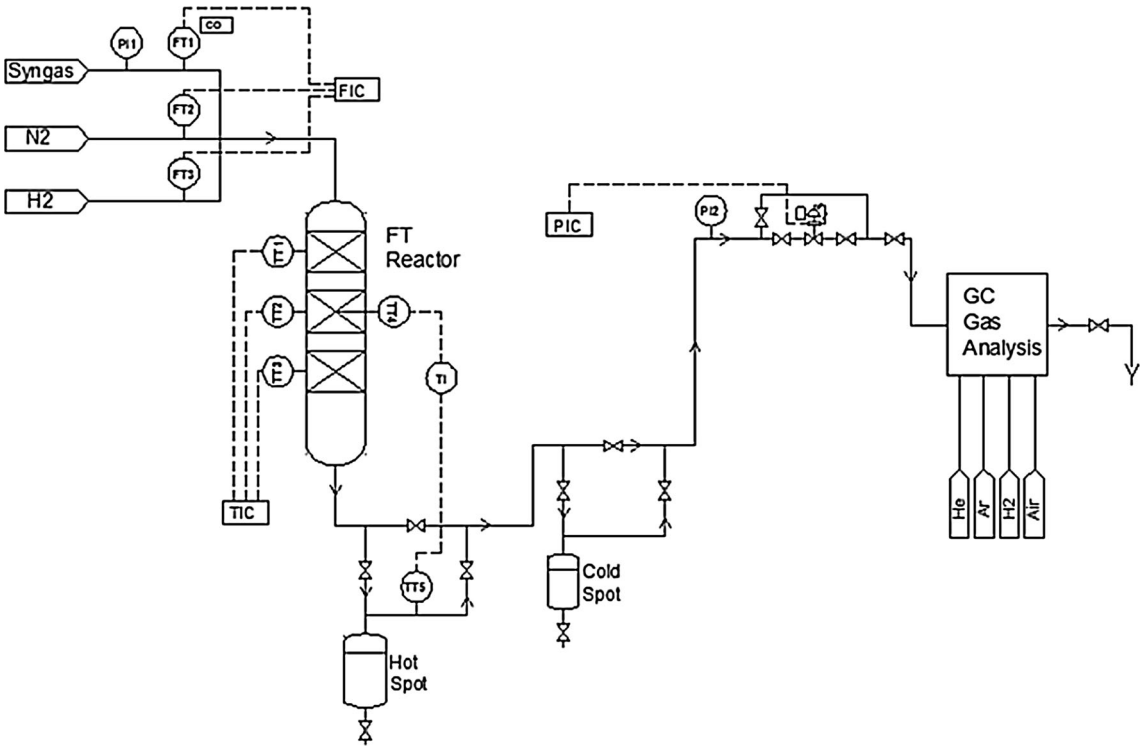

Fig. 1 Set-up of laboratory scale Fischer–Tropsch reactor

Table 2 Surface areas, pore volumes and pore diameters for the Al_2O_3-supported catalysts

Catalyst	BET surface area (m^2/g)	Pore volume (cm^3/g)	Average pore diameter (nm)
Al_2O_3	195	0.52	10.6
A20	117	0.31	10.8
A20Re0.2	125	0.31	9.7
A15Re0.2	126	0.34	10.8
A20Re1	106	0.26	9.8
A15Re1	121	0.29	9.4
A20Ru0.2	118	0.30	10.3
A15Ru0.2	133	0.36	10.7
A20Ru1	149	0.37	9.9
A15Ru1	124	0.31	10.0
SiC	29	0.15	24.0
S20	20	0.13	26.5
S20Re0.2	29	0.12	16.3
S15Re0.2	29	0.29	40.6
S20Ru0.2	22	0.14	26.4
S15Ru0.2	19	0.12	25.2
TiO_2	54	0.18	13.5
T20	25	0.23	36.6
T15Re0.2	29	0.12	16.3
T20Re0.2	30	0.24	33.0
T15Ru0.2	36	0.27	30.2
T20Ru0.2	38	0.28	29.8

this blockage is more severe for the smallest pores of the catalyst. This effect on the smallest pores can eventually be seen as an increase in mean pore sizes. Similar effects have also been reported in [12].

For the unpromoted catalysts the decrease in surface area is most obvious for the TiO_2 supported catalyst. In this case a 50 % decrease was observed, whereas the decrease for Al_2O_3 supported catalysts was 40 %.

Results from the CO chemisorption measurements are presented in Table 3 and as can be seen, dispersions of the active metal were low, for most of the catalysts in the range of 1–8 %). This low level of dispersion is typical for the cobalt catalysts and our results are consistent with those presented earlier [13]. Effect of addition of promoters is seen as increased dispersions and decreased particle sizes. According to the results in Table 3, the increase in dispersion seemed to be independent of the Co concentration, i.e. catalysts with 20 and 15 mass% Co have the same dispersion level. Instead, higher concentrations of promoter metals (1.0 mass% compared to 0.2 mass%) gave higher dispersions. This finding was only observed for Al_2O_3 based catalysts in the present study. A comparison between the supports reveals that the highest dispersions and smallest particle sizes are found on the Al_2O_3 based catalysts even if the catalyst T15Ru0.2 has a high level of dispersion.

The size of the cobalt particles was also measured by calculating the metal particle size from the XRD data using the Scherrer equation (Eq. 1). Due to the different approach compared to CO chemisorptions, there is some discrepancy between the results obtained. Particle sizes were not calculated for the Re or Ru promoted catalysts due to the small peaks obtained for these metals in the XRD diffraction patterns. The Co particle sizes calculated from the XRD data are in line with results published earlier [12, 14] and significantly smaller than particle sizes obtained from CO chemisorption.

Metal concentrations over Al_2O_3 supported catalysts are presented in Table 4. The measured concentrations are in line with the calculated concentrations even if they are slightly lower than expected. Furthermore, the concentrations of potassium and sodium in all analyzed catalysts are below the detection limit of the ICP method which is 5 mg/g. So we assume no or low amounts of K and Na are present in the samples. The concentrations of Na and K are even at the reported detection limit for the determinations below the concentrations reported [15, 16] to have a negative effect on the activity of the catalysts.

Table 3 Results from CO chemisorption measurements assuming a ratio of 2:1 between Co and CO

Catalyst	Co dispersion (%)	Co metal particle size (nm)	Co metal particle size (nm) from XRD	Co metal surface area (m^2/g of metal)
Al_2O_3				
A20	1.0	96	5.5	11
A20Re0.2	5.0	19		34
A15Re0.2	5.0	19		33
A20Re1	7.0	14		45
A15Re1	8.6	11		58
A20Ru0.2	n.d.	n.d.		n.d.
A15Ru0.2	2.2	44		14
A20Ru1	n.d.	n.d.		n.d.
A15Ru1	6.6	15		43
SiC				
S20	1.2	80	33	8
S20Re0.2	3.2	30		21
S15Re0.2	2.8	34		19
S20Ru0.2	2.0	48		13
S15Ru0.2	2.8	34		23
TiO_2				
T20	1.2	80	18	8
T15Re0.2	2.6	36		17
T20Re0.2	4.8	20		32
T15Ru0.2	7.6	12		51
T20Ru0.2	n.d.	n.d.		n.d.

Table 4 Metal concentrations in catalysts supported on Al_2O_3

Catalyst	Ru (mg/g)		Co (mg/g)	
	Calculated value	Measured value	Calculated value	Measured value
A20			200	190
A20Re0.2			200	180
A15Re0.2			150	150
A20Re1			200	170
A15Re1			150	120
A20Ru0.2	2	1.9	200	190
A15Ru0.2	2	1.6	150	140
A20Ru1	10	7.7	200	180
A15Ru1	10	7.7	150	140

3.2 XRD Analysis

XRD results for the Re promoted cobalt catalysts supported on Al_2O_3 are shown in Fig. 2a. Pure Al_2O_3 calcined at 420 °C for 16 h was used as a reference material and had a surface area of 195 m^2/g. The Al_2O_3 support material was proved to be γ-Al_2O_3 with a face-centered cubic phase Fd-3 m according to standard JCPDS card no. 00-50-0741 [16]. The 2θ peaks at 32°, 38°, 39° and 46° correspond to the (220), (311), (222) and (400) reflections of γ-Al_2O_3 respectively. The peaks of alumina were broad which denoted it is a nano-sized material whilst the calculated crystallize size from the XRD pattern was 8.1 nm for pure Al_2O_3.

The sample A20 with Co impregnation only has two high 2θ peaks at 36.8° and 42.7°, which correspond to CoO (111) and CoO (200) according to face-centered cubic CoO (Fm3 m) (JCPDS card no. 00-71-1178). There is also a shoulder between CoO (200) and Al_2O_3 (400), which may be caused by the (111) reflection of cubic cobalt (2θ of 44.3°) being merged with Al_2O_3 (400) (2θ of 45.7°) and CoO (200) (2θ of 42.8°). Therefore, we can assume the metal Co may also exist according to the Co pattern (JCPDS 04-014-0167).

For other catalysts samples containing the Re promoter Co (111) peak can be identified more easily. For A20Re1 and A15Re1 catalysts which have a higher Re content of 1 wt%, the peaks are overlapped and merged together while a larger shoulder can be identified between the CoO (111) and Al_2O_3 (400) peaks. However, Re reflections were difficult to identify because of the low concentration (≤ 1 wt%) and the strongest 2θ peak at 42.9° of Re (101) (JCPDS card no. 01-071-6589) mixing with CoO (200) at 42.4°.

For Ru promoted cobalt catalysts samples with Al_2O_3 supports, the XRD patterns were quite similar to the Re promoted samples (Fig. 2b). Both Co and CoO were presented in the samples because Co (111) and CoO (111) can be identified from the patterns. However, the peaks of Ru were difficult to identify because the concentration of Ru is relatively low (≤1 wt%) and the strongest peak of Ru (101) at 44.0° is mixing with Co (111) (2θ of 44.3°) according to JCPDS card no. 00-006-0663 of hexagonal Ruthenium.

XRD diffraction patterns for TiO2 supported catalyst samples are shown in Fig. 3. The pure TiO2 support material contains two phases which is a mixture of 85 wt% anatase with a body-centered tetragonal phase (JCPDS card no. 01-070-6826) and 15 wt% of rutile with its tetragonal phase (JCPDS card no. 01-089-4920). Calculated crystallize size from the XRD pattern was 16 nm for pure TiO2. The reflections of the strongest peak (111) of cubic cobalt (JCPDS card no. 04-014-0167) can be clearly observed at 44.3° for the four TiO2 supported catalyst samples. Re (101) with 2θ of 42.9° or Ru (101) at 44.0° were not identified due to their low concentration of Re.

XRD diffraction patterns for SiC supported catalysts are shown in Fig. 4. For pure SiC, the XRD patterns matches very well with hexagonal silicon carbide of JCPDS card no. 00-049-1428. It is clear to see the five peaks at 2θ of 34.1, 35.65, 38.1, 41.4 and 60.0 which corresponds to (101), (102), (103), (104) and (108) of the hexagonal silicate phases. Calculated crystallize size from Eq. (1) was 26 nm for pure SiC. For all the SiC supported cobalt catalysts samples, it is obviously that an observed peak at 2θ of 44.3° corresponds to Co (111), the highest peak of cubic cobalt, according to JCPDS card no. 04-014-0167. One small peak at 47.4° can also be detected and its intensity varied for different samples, which may correspond to the highest peak of hexagonal Co (101) according to JCPDS card no. 01-071-4239.

3.3 Activity and Selectivity of Catalysts

The catalysts A20Rul.0 and A20Ru0.2 were tested for activity and selectivity in the FTS as described in Sect. 2.3. After an initial stabilization period of 24 h with a flow of 250 ml/min the gas flow was reduced to give a conversion level of 50 % as calculated from the peak ratios of nitrogen

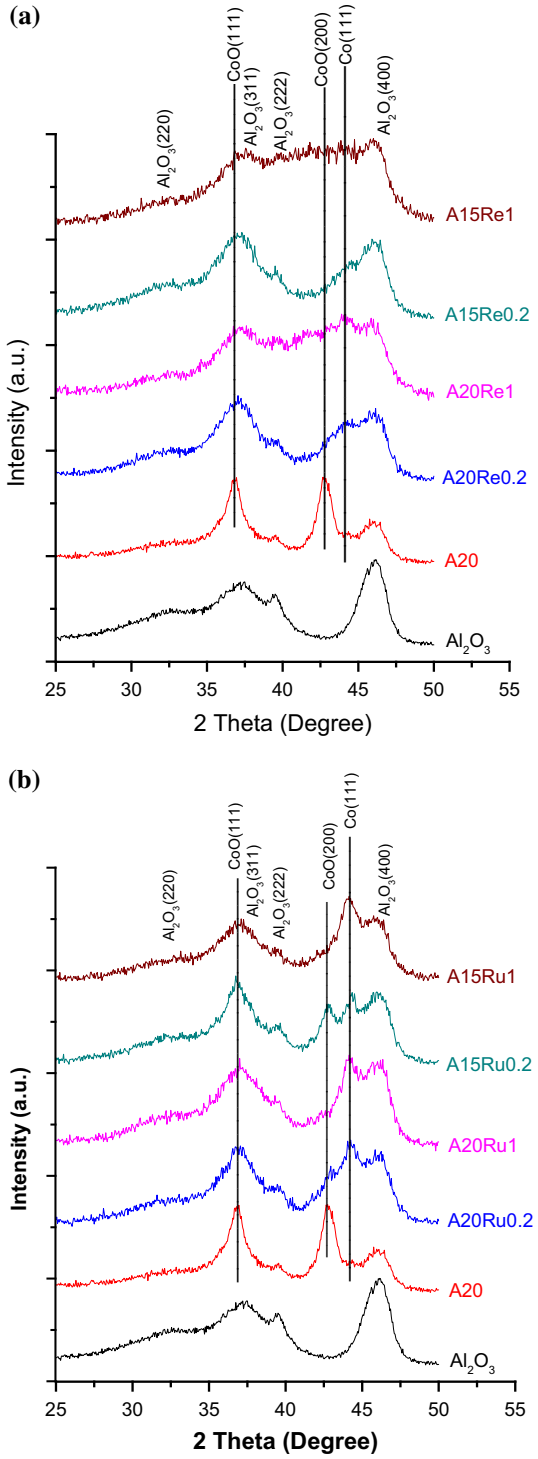

Fig. 2 XRD diffraction patterns of alumina supported cobalt catalysts with (**a**) Re promoter and (**b**) Ru promoter

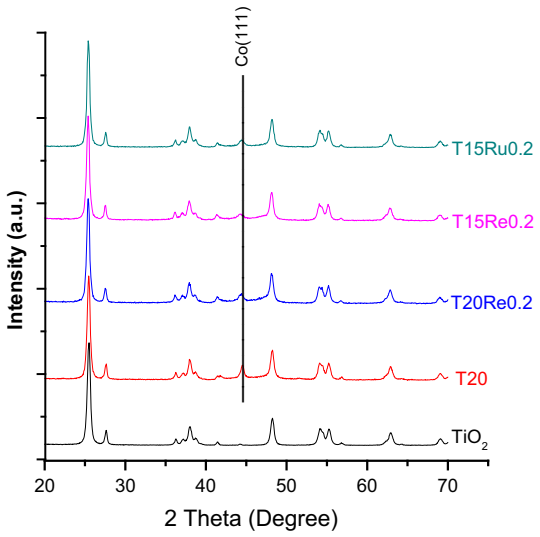

Fig. 3 XRD diffraction patterns for titanium oxide supported catalysts

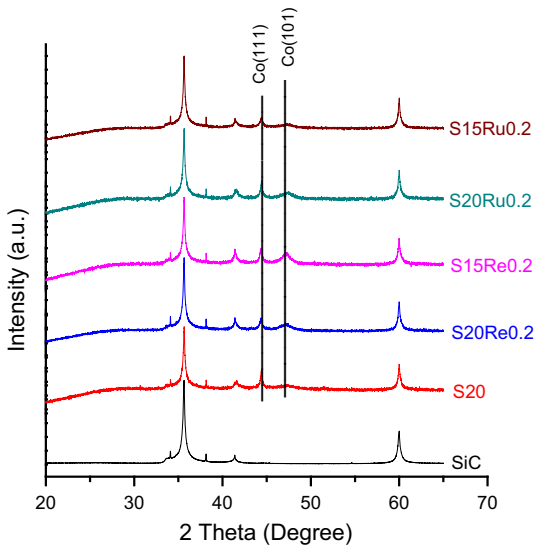

Fig. 4 XRD diffraction patterns for SiC supported catalysts

and carbon monoxide. Selectivity was calculated after 40 h of flow. The conversion levels and selectivities (C_{5+}) for the catalysts are presented in Fig. 5a and b respectively. For A20Rul catalyst the conversion level is still rising even after 45 h on stream and the selectivity for C_{5+} is slightly above 80 %. On the other hand, the A20Ru0.2 catalyst is almost stabilized after 45 h on stream with a conversion initially just over 50 %, which then drops slowly with further streaming. Although the selectivity for the later catalyst to C_{5+} is slightly higher than for the catalyst A20Rul, the selectivity is slowly decreasing but is never less than 80 % during the experiment.

Selectivity to methane (CH_4) was rather stable having a selectivity between 9.2 and 9.3 % for the catalyst A20Ru0.2, whereas the catalyst A20Rul had a significantly higher selectivity against CH_4 or 10.1–10.2 %.

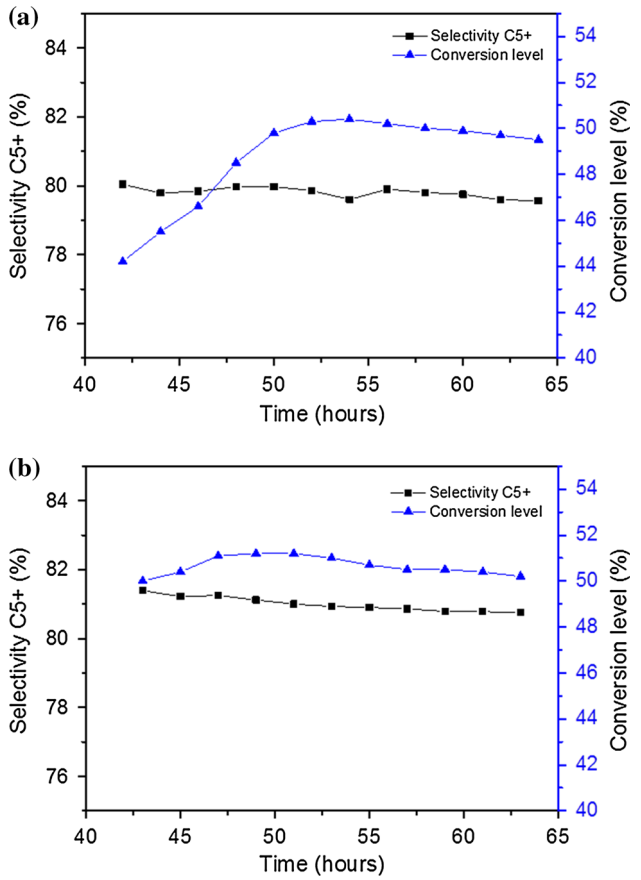

Fig. 5 Conversion level and selectivities to C_{5+} for the catalysts A20Rul (**a**) and A20Ru0.2 (**b**). *Right y axis* corresponds to the conversion level of CO (%), *left y axis* selectivity for C5+. *X axis*, time on stream (hours from start)

4 Conclusions

Normally studies are performed on one single support only. In this paper three different supports, alumina oxide (Al_2O_3), titanium dioxide (TiO_2) and silicon carbide (SiC) are used and compared. The cobalt catalysts are used as such or promoted by ruthenium (Ru) or rhenium (Re). Catalysts are characterized by a number of methods and two of the catalysts were tested for catalytic activity and selectivity in the Fischer–Tropsch reaction.

There is a significant effect of the addition of the different promoters on the cobalt particles formed, a similar effect can be seen between the different supports. This support dependent effect might be explained by the difference in pore size distributions of the supports used as explained by [16]. The Co particles produced for the promoted catalysts on all supports were in the region of 11-40 nm and for the unpromoted catalyst in the region of 80–96 nm. The particle sizes for all catalyst are in the region were the catalysts activity in the Fischer–Tropsch reaction is independent of the particle size. The dispersion of the metal particles is not as such a measure of the coming activity and selectivity properties of the catalysts. It is known that the activity of the catalysts in the Fischer–Tropsch reaction is dependent of the particle size for particle sizes less than 10 nm, for particles in the region of 10–100 nm in size the activity is independent of the particle size [17].

As a negative result addition of the active metal and promoter metals onto the support decreased the surface areas for all supports in the following order: $TiO_2 > Al_2O_3 > SiC$. The decrease in surface areas seems to be dependent on the amount of cobalt used. On the other hand, no obvious dependency between concentration of promoter metals and decrease in surface area was observed. The decrease in surface areas as a result of cobalt impregnation can be explained by a partial or total blockage of the pores, mainly the smallest pores of the catalyst. This effect on the smallest pores is most likely seen as an apparent increase in mean pore sizes especially in the SiC-supported catalysts.

The size of the cobalt particles was measured by two independent methods, i.e. chemisorption of CO and calculation of metal particle size from the XRD data using the Scherrer equation. Due to the different approaches in these two methods, there is some discrepancy between the results obtained. XRD data showed particle sizes from 5 to 33 nm for metallic cobalt depending on the support. For the Al_2O_3 supported catalysts, catalytic Fischer–Tropsch selectivities were measured to be around 80 % with the constant conversion level of 50 %.

Acknowledgments Authors would like to acknowledge the EU/Interreg Nord program (Project No. 304-8488-10) for its financial support within the HighBio2 project. The BRISK network and The Swedish Academy of Engineering Sciences in Finland are also acknowledged for awarding a Grant to H. Romar. Finally, many thanks go to Sasol, SiCat and Degussa for supplying the support materials.

References

1. Fiorese G, Catenacci M, Verdolini E, Bosetti V (2013) Advanced biofuels: future perspectives from an expert elicitation survey. Energy Policy 5(56):293–311
2. Khodakov AY, Chu W, Fongarland P (2007) Advances in the development of novel cobalt Fischer–Tropsch catalysts for synthesis of long-chain hydrocarbons and clean fuels. Chem Rev 107:1692–1744
3. Zhang W (2010) Automotive fuels from biomass via gasification. Fuel Process Technol 8(91):866–876
4. Tijmensen MJA, Faaij APC, Hamelinck CN, van Hardeveld MRM (2002) Exploration of the possibilities for production of Fischer–Tropsch liquids and power via biomass gasification. Biomass Bioenergy 8(23):129–152
5. Khodakov AY, Holmen A, Mirodatos C, Wang Y (2013) Catalysis and synthetic fuels: state of the art and outlook. Catal Today 215:1

6. Fiorese G, Catenacci M, Bosetti V, Verdolini E (2014) The power of biomass: experts disclose the potential for success of bioenergy technologies. Energy Policy 2(65):94–114
7. Hanaoka T, Liu Y, Matsunaga K, Miyazawa T, Hirata S, Sakanishi K (2010) Bench-scale production of liquid fuel from woody biomass via gasification. Fuel Process Technol 8(91):859–865
8. Ma W, Jacobs G, Keogh RA, Bukur DB, Davis BH (2012) Fischer–Tropsch synthesis: effect of Pd, Pt, Re, and Ru noble metal promoters on the activity and selectivity of a 25%Co/Al_2O_3 catalyst. Appl Catal A 437–438:1–9
9. Morales F, Weckhuysen BM (2006) Promotion effects in Co-based Fisher–Tropsch catalysis. Catalysis 19:1
10. Hackley VA, Stefaniak AB (2013) ''Real-world'' precision, bias, and between-laboratory variation for surface area measurement of a titanium dioxide nanomaterial in powder form. J Nanopart Res 15(1742):1–8
11. International Centre for Diffraction Data (ICDD) (2013) PDF-4 + powder diffraction database. 12 Campus Boulevard Newton Square, PA 19073-3273, USA
12. Hosseini SA, Taeb A, Feyzi F, Yaripour F (2004) Fischer–Tropsch synthesis over Ru promoted Co/γ-Al_2O_3 catalysts in a CSTR. Catal Commun 3(5):137–143
13. Iglesia E (1997) Design, synthesis, and use of cobalt-based Fischer–Tropsch synthesis catalysts. Appl Catal A 161:59–78
14. Storsæter S, Borg Ø, Blekkan EA, Holmen A (2005) Study of the effect of water on Fischer–Tropsch synthesis over supported cobalt catalysts. J Catal 231:405–419
15. Lillebø AH, Patanou E, Yang J, Blekkan EA, Holmen A (2013) The effect of alkali and alkaline earth elements on cobalt based Fischer–Tropsch catalysts. Catal Today 215:60–66
16. Blekkan EA, Holmen A, Vada S (1993) Alkali promotion of alumina-supported cobalt Fischer–Tropsch catalysts studied by TPR, TPD and pulse chemisorption. Acta Chem Scand 47:275–280
17. Borg Ø, Dietzel PDC, Spjelkavik AI, Tveten EZ, Walmsley JC, Diplas S et al (2008) Fischer–Tropsch synthesis: cobalt particle size and support effects on intrinsic activity and product distribution. J Catal 259:161–164